2016 49th Hawaii International Conference on System Sciences

# Assessing risk of gas shortage in coupled gas-electricity infrastructures

Anatoly Zlotnik
*Center for Nonlinear Studies*
*Los Alamos National Laboratory*
*Los Alamos, NM*
*azlotnik@lanl.gov*

Michael Chertkov
*Theoretical Division*
*Los Alamos National Laboratory*
*Los Alamos, NM*
*chertkov@lanl.gov*

Konstantin Turitsyn
*Department of Mechanical Engineering*
*Massachusetts Institute of Technology*
*Cambridge, MA*
*turitsyn@mit.edu*

***Abstract*—Many power systems in the United States and elsewhere are experiencing simultaneous increases of the gas-fired and renewable portions in the generation profile. Both contributions are sufficiently clean to replace retiring generators, which are mainly coal-fired. Moreover, pairing gas and renewables is advantageous because the former is flexible enough to mitigate the exogenous fluctuations of the latter. However, the resulting strong coupling of power systems and gas transmission networks through gas-fired generators also imposes risks. In particular, excessive fuel usage by gas-fired power plants may lead to violation of gas pressure limits and gas supply shortages. To provide a simple tool for assessing these risks, we develop a computational framework that characterizes regions of generator dispatch solutions that maintain gas system feasibility. The proposed algorithmic framework is modular – built through a coordinated execution of multiple generation scenarios within power and gas simulation modules. Monotone dependence of the gas pipeline pressure on the rates of gas withdrawals allows to establish and certify regions of feasibility/infeasibility in the space of the gas injections. The framework is validated against simulations of a highly detailed benchmark gas-electricity model. We conclude the manuscript with a discussion of possible applications of the results to power system operation procedures and regulatory practices.**

***Keywords*-Natural Gas Networks; Gas-Electric Coupling; Optimal Power Flow**

## I. Introduction

Many regional authorities in the world have adopted aggressive plans for introducing high amounts of clean and sustainable resources to the energy mix [1], [2]. However, the intermittent and uncontrollable nature of these resources has become a major concern for power industry practitioners tasked to maintain an almost instantaneous balance between generation and consumption [3]. At the same time, the retirement of many coal-fired generators and the decreasing cost of natural gas, coupled with improvements in the overall efficiency of gas turbines, has created an opportunity for gas-fired generation technology. Moreover, from the operational perspective, gas turbines are characterized by high maneuverability, and hence are the most suitable resources to balance the fluctuations of renewable power. In combination, these considerations make the gas fired generation the most economic bridge from the existing power systems to lower-carbon and secure future systems [4].

However, and despite all its advantages, gas-fired generation is by no means a silver bullet for resolving the renewable intermittency problem. Indeed, reliance on gas-fired generation in the presence of substantial fluctuations and unpredictability only shifts the problem of energy balance to the natural gas pipeline infrastructure [5], [6]. Natural gas is moved over transmission pipeline systems spanning thousands of miles with a typical speed of 10 to 15 m/s, thus making delivery a relatively slow and inertial processes. Therefore actions, e.g. by the gas producer at the head of the line, and consequences, e.g. for a customer at the end of the line, are separated by tens of hours. Although the ability to pack fuel in a pipeline somewhat mitigates the effective "inertia" of the system, such operations are currently conducted in an ad-hoc, suboptimal manner. Furthermore, unexpected fluctuations of fuel demand may result in shortages of natural gas, resulting in an inability of the gas-fired generation to balance power flow in the electric grid [7], [8], [9].

Although these risks are widely recognized by the power systems community [10], they have not yet been properly assessed by Independent System Operators (ISOs). Rigorous analysis of these risks is an extremely challenging interdisciplinary problem. Northern countries with significant penetration of wind generation, where the natural gas is also commonly used for heating purposes, are especially prone to the risks associated with often violent and hard to predict day-to-day changes in wind and weather patterns. Operation of modern gas pipeline networks may require adherence to regulations and procedures, which are especially strict and constrained in the events of extreme cold. Direct modeling of such operations can be difficult, especially in the presence of limited coordination between gas and electricity operators [11]. Recently, tractable modeling and control frameworks accurately representing physical phenomena in gas pipelines [12] and networks [13] were developed. These reduced control system models enable fast simulation and optimization of dynamic compressible gas flows over systems with nodal controllers, providing unprecedented gains in efficiency and scalability. Such techniques have enabled the extension of the steady-state optimal gas flow (OGF) [14], [15] to the dynamic case [13]. In the dynamic regime,

1530-1605/16 $31.00 © 2016 IEEE
DOI 10.1109/HICSS.2016.315

the partial differential equation (PDE) representation of a gas pipeline network is approximated by a new simulation and control system model called the reduced network flow (RNF), which was validated using traditional numerical PDE solution methods [12].

Despite these advances in modeling and analysis capabilities, full co-optimization and even co-simulation of the two infrastructures may not be possible in the near future for at least two major reasons. First, the lack of regulatory policies to require coordination between the gas and electricity sectors limits the data exchange and overall cooperation between operators of the two infrastructure systems. Moreover, the nonlinear and high-dimensional nature of the models limits the range of tools available for operational coordination. In this work, we address these challenges and propose a novel modular simulation-based risk assessment methodology. Specifically, we develop an algorithmic framework to characterize a set of the feasibility domains (in the proper phase space) of the gas system operation. This set of domains have a simple geometrical interpretation and can thus be used naturally by ISOs to assess the risks of gas shortages, in particular related to the presence of widespread penetration of highly variable, intermittent, and poorly predictable renewable energy sources.

An important feature of the proposed methodology is its modular structure, which is based on coordinated execution of three independent simulation modules. The first "scenario generation module" is responsible for sampling of possible renewable generation scenarios. This module can potentially generate scenarios based on stochastic models of weather, component outages, as well as fluctuations in load and generation. This module is coupled with the "power grid simulation module", which approximates power dispatch as it is implemented in the power grid. A particular outcome of the power grid simulation module is a collection of time-varying functions describing the rates of fuel consumption by the gas-fired power plants. This information is passed to the (third) "gas network simulation module", which emulates the behavior of the gas pipeline system. The third module incorporates important details of the gas system technological procedures such as compressor control. Crucially, all of the modules can be supplied to ISOs by external vendors and do not require any critical data sharing. Coordinated execution of the modules as proposed in this work allows fast reconstruction of the set of feasibility domains. Knowledge of this set enables an accurate characterization of gas supply disruption risks even in the more challenging situations when these risks are moderate or small and thus difficult to assess via naive approaches.

To reduce simulation time and efficiently compute the desired certificates, we exploit a special "component-monotonicity" (or simply monotonicity) property of the gas flow equations, which is inherited from a more general monotonicity property of dissipative flows over networks

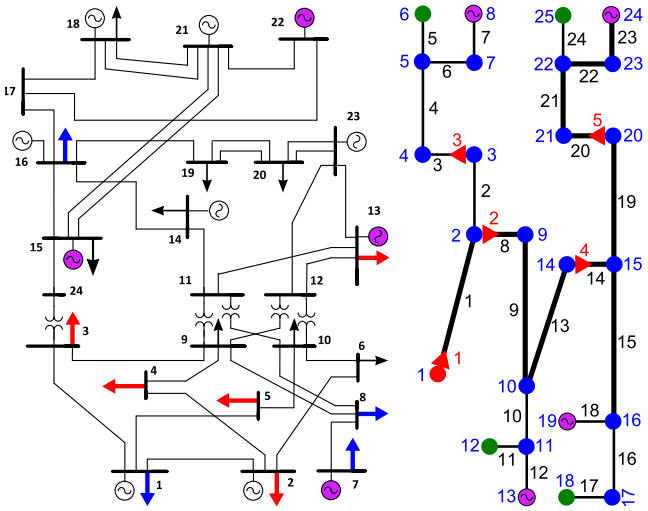

Figure 1. Left: IEEE One Area RTS-96 system [18] with gas generators (purple), constant loads (black arrows), time-varying loads for high PV (red arrows) and standard (blue) as in Figure 2. Right: Gas pipeline test network. Numbers indicate nodes (blue), edges (black), and compressors (red). Thick and thin lines indicate 36" and 25" pipes. Nodes are source (red), transit (blue), consumers (green), and gas generators (purple).

[16], [17]. The monotone dependence of pipeline gas pressure on consumption levels was demonstrated as a network-wide property, and has been invoked to greatly reduce the computational cost of optimization problems for compressible gas network flows [16]. Originally considered in the quasi-static case, the property also allows dynamic generalization. This key property provides an opportunity to certify feasibility of a whole range of operating conditions using only two simulations for the extremal cases. The proper exploitation of this idea results in an efficient algorithm for establishing the feasibility set in the gas-power injection space. Naturally, these regions can be incorporated in ISO decision making processes such as unit-commitment analysis or security assessment.

This manuscript is organized as follows. Section II describes the gas-electricity infrastructure coupling model. Section III presents the algorithm – the key contribution of the manuscript. The performance of the algorithm is then validated, and simulation results are presented in Section IV. Section V is reserved for conclusions, as well as discussion of applications of the proposed framework and suggested future research directions.

## II. Description of Gas-Grid Model

In this section, we describe techniques for simulating the behavior of integrated electric power and natural gas infrastructures, and their application to a model consisting of test networks for power and gas systems, with 24 and 25 nodes, respectively, and which are coupled through gas-fired generators.

### A. Electric Power and Gas System Networks

We use the IEEE One Area RTS-96 test network [18] in Figure 1 for our simulation studies. The model is scaled such that total generation capacity is 2724 MW, and line capacities and system loads are reduced to 50% and 80% of nominal values, respectively. Certain loads are scaled according to the time-varying curves in Figure 2 associated with standard loads (blue) and high photovoltaic (PV) penetration (red). The remaining constant electric loads are scaled to 25% of nominal values. Gas-fired shoulder plants are located at buses 7 and 13, and peak power plants are placed at 15 and 22. The costs $c(p_i) = c_g q(p_i)$ of operating these units at outputs $p_i$ are functions of gas usage, given by

$$q(p_i) = q_0 + q_1 p_i + q_2 p_i^2. \tag{1}$$

The quadratic cost coefficients are $(q_0, q_1, q_2) = (3.08, 0.48, 0.001)$ for peaking plants and $(7.83, 0.26, 0.0015)$ for shoulder plants [19], and are taken from MatPower for the remaining loads [20]. The cost of gas is set to an invariant value of $c_g = 6$ \$/mmBTU. The generators use fuel from the gas pipeline test network shown in Figure 1. The friction factor and sound speed parameters are $\lambda = 0.01$ and $a = 377.968$ m/s. Gas-fired units at power system nodes 22,15,13, and 7 draw fuel from gas system nodes 8, 13, 24, and 19, respectively. In the integrated model the generators use approximately 30% of the gas, and approximately 40% of gas is used for power. The consumers at gas system nodes 6, 12, 18, and 25 each use the rest of the gas at an average rate of 40 kg/s, scaled by the standard time-varying demand profile in Figure 2. Gas is injected onto the network at node 1 at 500 psi, and boosted into the system by compressor 1. The total amount of gas transferred through the system is approximately 500,000 mmBTU/day. The nodal pressures are nominally constrained to lie within $[500, 800]$ psi, and compression ratios are bounded on the interval $[1, 2]$ when computing the OGF.

### B. Gas Generator Fuel Use From Electric Power Loads

We first review how day-ahead electricity market forecasts are used to predict fuel usage profiles of gas-fired generators. ISOs such as PJM [21] or ISO-New England [22] clear the market by solving optimal power flow (OPF) and unit commitment problems [23] to produce hourly generation schedules for the following day. A simple approximate prediction of gas-fired unit fuel consumption is given by solving an OPF for which demand forecasts and production are continuous functions of time. We use the DC power flow approximation, which is in line with previous integration studies [24], [25], [26], [27], [28]. For simplicity, we disregard any constraints related to line outages, time-coupling constraints for ramping or unit commitment in the current OPF formulation.

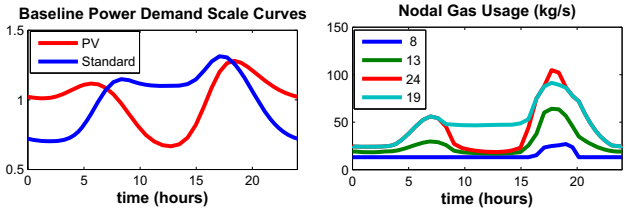


Figure 2. Left: Normalized electricity demand profiles. Right: Gas-fired generator fuel use from solving the DC OPF (7) for the baseline deterministic case and applying (1).

The continuous-time DC OPF is formulated as an extension to the standard single time-step problem [29]. Let $\mathbb{G}_P = (\mathcal{V}_P, \mathcal{E}_P)$ represent the power network graph, where $\mathcal{V}_P$ is the set of nodes with $|\mathcal{V}_P| = m$ and $\mathcal{E}_P$ is the set of lines of the system with $|\mathcal{E}_P| = n$. The set of generators is denoted by $\mathcal{G}$. We assume for simplicity that there is one generator with production $p_i(t)$ and one demand with consumption $h_i(t)$ per node, such that $|\mathcal{G}| = |\mathcal{V}_P| = m$. The demands $h_i(t)$ are given as continuous demand functions defined for $0 \le t \le T$ where $T = 24$ hours. Power flows from bus $i$ to bus $j$ are denoted by $f_{ij}$, with maximum values of $\bar{f}_{ij}$. We wish to minimize the cost of generation over the time interval $[0, T]$ where $c_i(p_i(t))$ are cost functions for production. This takes the form

$$J_P \triangleq \sum_{i \in \mathcal{G}} \int_0^T c_i(p_i(t)) \mathrm{d}t. \tag{2}$$

The constraints for total system power balance, generator production limits, and power flow limits at all times are

$$\sum_{i \in \mathcal{V}} (p_i(t) - h_i(t)) = 0, \quad \forall t \in [0, T] \tag{3}$$

$$0 \le p_i(t) \le p_i^{max}, \quad \forall i \in \mathcal{G}, \quad \forall t \in [0, T] \tag{4}$$

$$-\bar{f}_{ij} \le \mathbf{M}_{(ij,\cdot)}(p(t) - h(t)) \le \bar{f}_{ij}, \ \forall \{ij\} \in \mathcal{E}_P, \ \forall t \in [0, T] \tag{5}$$

where $p(t)$ and $h(t)$ are vector functions containing $p_i(t)$ and $h_i(t)$, respectively. The matrix $\mathbf{M} \in \mathbb{R}^{n \times m}$ relates the line flows to the nodal power injections, and is defined as

$$\mathbf{M} = B_f \begin{bmatrix} (\widetilde{B}_{bus})^{-1} & \mathbf{0} \\ \mathbf{0} & 0 \end{bmatrix} \tag{6}$$

where $B_f$ and $\widetilde{B}_{bus}$ are line and bus susceptance matrices, where the column and row corresponding to the slack bus are omitted from $\widetilde{B}_{bus}$ [30]. $\mathbf{M}_{(ij,\cdot)}$ is the row of $\mathbf{M}$ related to line $(ij) \in \mathcal{E}_P$. The continuous-time DC OPF is then given by

$$\begin{aligned} \min_{p(t)} \quad & J_P \text{ in (2)} \\ s.t. \quad & \text{power system constraints: (3)} - \text{(5)} \end{aligned} \tag{7}$$

The functional optimization problem (7) is solved using a pseudospectral collocation scheme [31], [13] using 50 collocation points in time. The computation is implemented by building functions for the objective, constraints, and their

gradients with respect to the decision variables (the polynomial coefficients). These are given, along with random initial conditions that satisfy inequality constraints, to the interior-point solver IPOPT version 3.11.8 running with the linear solver ma57 [32]. The generation and fuel usage of gas-fired units for the base stress case are shown in Figure 2. In the following section, we describe how the effects of these withdrawals on the gas pipeline network are simulated.

### C. Simulation of Gas Network Dynamics

We use a reduced control system model for gas pipeline networks actuated by nodal compressor stations [13] to simulate the effect of wind variability on gas transmission systems. Such systems are represented by directed graphs $\mathbb{G} = (\mathcal{V}, \mathcal{E})$, where each edge $\{i, j\} \in \mathcal{E}$ connects nodes $i, j \in \mathcal{V}$. The state on an edge $\{i, j\}$ is defined by the density $\rho_{ij}$ and flux $\varphi_{ij}$ on a time interval $\mathcal{T} = [0, T]$ and the distance variable $x_{ij} \in [0, L_{ij}] = \mathcal{L}_{ij}$, where $L_{ij}$ is the length of edge $\{i, j\}$. Under the conditions experienced by gas transmission systems, in which the flows do not undergo waves or shocks, the density and flow dynamics on the edges are well-approximated by a simplification of the Euler PDE equations in one dimension [33], [34], [35], given after nondimensionalization [13] by

$$\partial_t \rho_{ij} + \partial_x \varphi_{ij} = 0, \qquad \forall \{i, j\} \in \mathcal{E} \tag{8}$$

$$\partial_t \varphi_{ij} + \partial_x \rho_{ij} = -\frac{\lambda_{ij}\ell}{2D_{ij}} \frac{\varphi_{ij}|\varphi_{ij}|}{\rho_{ij}}, \qquad \forall \{i, j\} \in \mathcal{E}. \tag{9}$$

This, in addition to flow balance conditions at junctions, characterizes the unperturbed flow dynamics throughout the network.

Because friction causes the pressure of gas flowing through a pipeline to gradually decrease, compressors are used to boost gas pressure and maintain flow. This action is modeled as conservation of flow and a multiplicative change in density at a point $x = c$ with the compression ratio $\alpha(t)$. The required power is proportional to

$$C \propto \eta^{-1} |\varphi(t, c)| (\max\{\alpha(t), 1\}^{2m} - 1) \tag{10}$$

with $0 < m < (\gamma - 1)/\gamma < 1$ where $\gamma$ is the heat capacity ratio and $\eta$ is the compressor efficiency [14], [15]. Compressors are defined on a set $\mathcal{C} \subset \mathcal{E} \times \{+, -\}$, where $\{i, j\} \equiv \{i, j, +\} \in \mathcal{C}$ denotes a controller located at node $i \in \mathcal{V}$ that augments the density of gas flowing into edge $\{i, j\} \in \mathcal{E}$ in the $+$ direction. Compression is then modeled as a multiplicative ratio $\alpha_{ij} : \mathcal{T} \to \mathbb{R}_+$ for $\{i, j\} \in \mathcal{C}$. We denote by $s_j : \mathcal{T} \to \mathbb{R}$ the density of gas entering the network from a node $j \in \mathcal{V}_S$, where the set $\mathcal{V}_S$ denotes large supply terminals we call "slack" junctions, able to supply any mass flux at the given density. A mass flux withdrawal (or injection, if negative) at a junction $j \in \mathcal{V}_D = \mathcal{V} \setminus V_S$ is denoted by $d_j : \mathcal{T} \to \mathbb{R}$, where $\mathcal{V}_D$ is the set of demand (non-"slack") nodes.

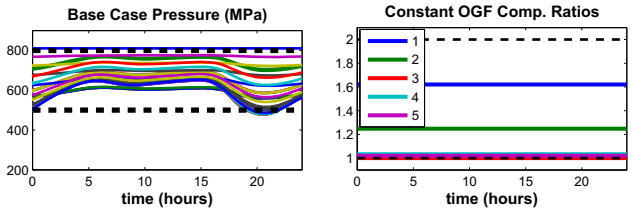


Figure 3. Left: Simulated nodal pressures (color) and pressure bounds (dashed); Right: Compression ratios computed using the OGF solved with gas usage multiplied by an engineering factor of 1.55 (1.62,1.25,1,1.03,1.02)

Suppose that $V = |\mathcal{V}_D|$ and $E = |\mathcal{E}|$, and assign to each edge an index in $[E]$, where $[N] = \{1, \ldots, N\}$ for a positive integer $N \in \mathbb{N}$, using the mapping $\pi_e : \mathcal{E} \to [E]$. Each node in $\mathcal{V}_D$ is assigned a unique internal density and each edge in $\mathcal{E}$ is assigned a flow, yielding the nodal density and edge flow state vectors $\rho = (\rho_1, \ldots, \rho_V)^T$ and $\varphi = (\varphi_1, \ldots, \varphi_E)^T$. We define the collection of nodal withdrawal fluxes $d = (d_1, \ldots, d_V)^T$, where $d_j$ is negative if an injection. Also define the slack node densities as $s = (s_1, \ldots, s_b)^T$, where $b = |\mathcal{V}_S|$. Define the diagonal matrices $\Lambda, K \in \mathbb{R}^{E \times E}$ by $\Lambda_{kk} = L_k$ and $K_{kk} = \ell \lambda_k / D_k$, where $L_k$, $\lambda_k$, and $D_k$ are the nondimensional length, friction coefficient, and diameter of edge $k = \pi_e(ij)$.

We then define the time-dependent weighted incidence matrix $B : \mathbb{R}^{|\mathcal{E}|} \to \mathbb{R}^{|\mathcal{V}|}$ by

$$B_{ik} = \begin{cases} \alpha_{ij} & \text{edge } k = \pi_e(ij) \text{ enters node } i, \\ -\alpha_{ij} & \text{edge } k = \pi_e(ij) \text{ leaves node } i, \\ 0 & \text{else} \end{cases} \tag{11}$$

as well as the incidence matrix $A = \text{sign}(B)$. Let $A_s, B_s \in \mathbb{R}^{b \times E}$ denote submatrices of rows of $A$ and $B$ corresponding to $\mathcal{V}_S$, and let $A_d, B_d \in \mathbb{R}^{V \times E}$ correspond similarly to $\mathcal{V}_D$. Define the function $g : \mathbb{R}^E \times \mathbb{R}^E_+ \to \mathbb{R}^E$ by $g_j(x, y) = x_j |x_j| / y_j$. The reduced network flow model is given by

$$\dot{\rho} = (|A_d| \Lambda |B_d^T|)^{-1} [4(A_d \varphi - d) - |A_d| \Lambda |B_s^T| \dot{s}], \tag{12}$$

$$\dot{\varphi} = -\Lambda^{-1} (B_s^T s + B_d^T \rho) - K g(\varphi, |B_s^T| s + |B_d^T| \rho). \tag{13}$$

For a connected graph, $A_d \in \mathbb{R}^{V \times E}$ and $B_d \in \mathbb{R}^{V \times E}$ are full rank, and therefore $|A_d| \Lambda |B_d^T|$ is invertible. Time-varying parameters are gas withdrawals $d \in \mathbb{R}^V$, input densities $s \in \mathbb{R}^b_+$, and compressions $\alpha_{ij} \in \mathcal{C}$. We note that in the steady state, equations (12)-(13) reduce to the static balance laws [15], [13].

We use the above model to simulate the gas network dynamics resulting from the optimization in Section II-B. The fuel usage profiles in Figure 2 are averaged, then multiplied by an engineering factor of 1.55 to compensate for using quasi-steady modeling to optimize a dynamical system. A steady-state OGF [15] is solved to yield constant compression ratios. This type of naive optimization roughly mimics current operating practices in the gas transmission industry. The optimization is implemented using the interior-point

solver IPOPT version 3.11.8 running with the linear solver ma57 [32], using the steady-state Weymouth equations and nodal flow balance conditions [15], [36]. These compressor protocols and the reduced network flow equations (12)-(13) determine gas network dynamics over the following 24-hour period, which are simulated using the low-order solver `ode15s` for stiff ODE systems in MATLAB. For the test network in Section II, the entire procedure terminates in seconds, and the results are shown in Figure 3.

Computationally, in order to analyze pressure constraint violations in the gas system, we compute the $L_2$ norm of these violations. The latter is of the form

$$V_{\rho}=\left[\int_0^T (p(t)-p_{\max})_+^2 \mathrm{d}t\right]^{\frac{1}{2}}+\left[\int_0^T (p_{\min}-p(t))_+^2 \mathrm{d}t\right]^{\frac{1}{2}} \tag{14}$$

where $(x)_+ = x$ if $x \geq 0$ and $(x)_+ \equiv 0$ if $x < 0$. When computing this norm, we consider violations outside of the interval $[p_{\min}, p_{\max}]$, for which we use $[450, 850]$ psi. Whenever the norm $V_{\rho}$ is non-zero the solution is infeasible.

## III. Gas Supply Disruption Risk Assessment Algorithm

As described in the previous section, the feasibility region of the gas flow equations is defined by the set of constraints $p_{\min} \leq p(t) \leq p_{\max}$ at the nodes of the pipeline network. We perform the comparison of the vectors component-wise, so we say that $a \geq b$ if $a_k \geq b_k$ for all indices $k$.

The values of gas pressure are determined by the time-dependent vector of gas withdrawals $d(t)$ at the gas terminals at major heating gas consumers as well as gas-fired power-plants. The exact dependence of the pressure on the gas consumption vector is complicated and depends on the compressor control policies employed by the gas network operator. Feasibility of pressure constraints is achieved in a generally non-convex region in the gas withdrawal vector space. Characterization of the feasible gas withdrawal region is essential for gas-infrastructure aware decision making processes on the power grid side and is the subject of this study.

Although the full dependence of gas pressure on withdrawal rates is very complicated, it can be shown to be monotonic [16]. Monotonicity is a critically important property of the system and lies at the foundation of the algorithm developed in this work. Simply speaking, monotonicity implies that all the sensitivities $\partial p_i(t)/\partial d_j(t') \leq 0$ for $t \geq t'$ of the gas pressure to consumption levels are negative. In other words, increase in the gas withdrawal rate can only result in decrease of the gas pressure at all locations in the pipeline network.

This property is seemingly natural, however it does not hold for all of the traditional infrastructure networks. In power systems, for example, increasing the power consumption can in fact lead to unloading of some lines in situations where the power grid has loops. However, physical laws describing the mass transport through gas infrastructure ensure that this property is satisfied for gas networks, at least for most natural and common compressor control policies.

Monotonicity of the dependence of pressure on gas consumption implies that whenever the set of constraints $p \leq p_{\max}$ is satisfied for some gas consumption vector $d$, it is also satisfied for all $d' \geq d$. Similarly, whenever $p \geq p_{\min}$ is valid for some $d$, it is also valid for all $d' \leq d$. This observation dramatically simplifies the analysis of robustness and forms the foundation of the algorithm developed in this work. The key idea of the algorithm is to use the monotonicity property to establish certificates for the existence of feasible solutions in the entire region of possible gas withdrawals. Whenever the regions established by the algorithm are large enough to cover most of the scenarios of interest, feasibility of these scenarios can be established by simply ensuring that the scenarios belong to a the region without running computationally expensive gas flow simulations. Similarly, regions of infeasibility where the solutions to the gas flow equations are provably infeasible can be used for quick analysis of the scenarios that lie outside of feasible region.

There are multiple ways to approximate the feasibility and infeasibility regions of gas flow solutions explained in the previous paragraph. In this work we discuss only one, simple approach to this problem. We assume that the gas flow simulation module acts as a "feasibility oracle" that answers the question of whether a given gas withdrawal trajectory $d(t)$ results in a feasible solution of the dynamic power flow equations. Access to such an oracle allows one to construct whole regions of feasible and infeasible solutions of monotone systems. Multiple regions can be constructed, each of which corresponds to a given feasible withdrawal vector $d$. In a similar fashion to how loadability limits are computed for power systems, it is possible to define the limits of gas withdrawal loadability for gas infrastructures. If the gas withdrawal rates at every node and every moment of time are increased proportionally by a scalar factor of $\lambda > 0$, the feasibility of the solution will be violated once the value of $\lambda$ exceeds the critical value $\overline{\lambda}$. Similarly, decreasing the gas withdrawal rate can raise the pressure beyond acceptable levels, which leads to a lower bound $\underline{\lambda}$. Given the values of $\overline{\lambda}$ and $\underline{\lambda}$, one can establish three feasibility certificates. First, whenever the vector $d'$ belongs to the polytope $\underline{\lambda} d \leq d' \leq \overline{\lambda} d$ the solution corresponding to withdrawal vector $d'$ is provably feasible. Second, whenever the gas withdrawal vector $d'$ satisfies one of the inequalities $d' > \overline{\lambda} d$ or $d' < \underline{\lambda} d$, the solution to gas flow equations is provably infeasible. These facts follow directly from the monotonic dependence of the pressure on gas flow consumption vector.

There are many ways of finding the critical values $\overline{\lambda}$ and $\underline{\lambda}$. Whenever the gas flow simulator module is represented by a feasibility oracle, the simplest algorithm of finding the critical values of $\overline{\lambda}$ and $\underline{\lambda}$ is the well known bisection method.

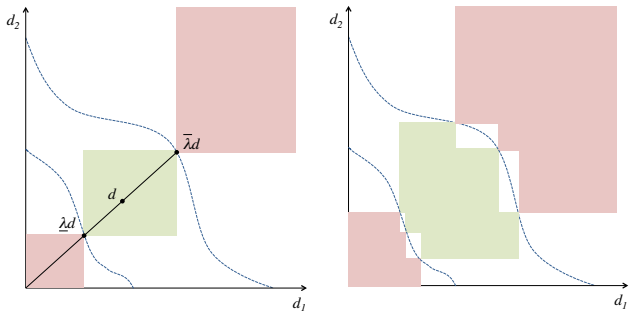


Figure 4. Left: Abstract schematic of the feasibility and infeasibility region construction. Dashed curve illustrates the actual boundaries of feasible region. The green region represent the polytope certified to be feasible via monotonicity criterion. Red regions are provably infeasible. Right: Schematic representation of the union of feasible/unfeasible sets.

This method forms a sequence of intervals $[\lambda_t^{\min}, \lambda_t^{\max}]$ that provably contains the value of $\overline{\lambda}$ and decreases in length as $t \to \infty$. Assume that the value of $\lambda = 1$ belongs to the feasible region. Then, one can use a geometric progression $\lambda_t = r^t$ with $r > 1$ to find two value of $\lambda_0^{\min} = r^{t-1}$ and $\lambda_0^{\max} = r^t$ that satisfy the property that $\lambda_0^{\min}$ belongs to the feasible region, while $\lambda_0^{\max}$ is already in an infeasible region. Once such a pair is found the algorithm proceeds via a standard bisection iteration. On every step the feasibility of the gas consumption vector corresponding to the value of $\lambda_t^* = (\lambda_t^{\min} + \lambda_t^{\max})/2$ is assessed via a feasibility oracle. If $\lambda_t^*$ belongs to the feasible region we set $\lambda_{t+1}^{\min} = \lambda_t^*$ and keep $\lambda_{t+1}^{\max} = \lambda_{t+1}^{\max}$. Otherwise, we set $\lambda_{t+1}^{\max} = \lambda_t^*$ but keep $\lambda_{t+1}^{\min} = \lambda_t^{\min}$. This way the true value of $\overline{\lambda}$ always belongs to the interval, and its size decreases in an exponential manner. The number of steps necessary to estimate the value of $\overline{\lambda}$ therefore scales logarithmically with the inverse accuracy of the estimate. A similar procedure can be naturally applied to the estimation of $\underline{\lambda}$.

Although the feasibility regions constructed for any individual gas withdrawal scenario $d$ may be large enough to certify feasibility of small variations on top of a given scenario, sufficiently different scenarios may need to be certified separately. Fortunately, the simple structure of the feasible regions allows for straightforward aggregation of multiple regions constructed via simulations. Assume that $n$ scenarios have been analyzed, leading to critical polytope vertices denoted as $\overline{d}^{(k)} = \overline{\lambda}^{(k)} d^{(k)}$ and $\underline{d}^{(k)} = \underline{\lambda}^{(k)} d^{(k)}$, with the upper index $k = 1 \ldots n$ corresponding to different scenarios. By definition, the union of feasible regions is also feasible, so the generation of multiple regions is a natural way to extend the certified region. To check whether a given point $d$ belongs to the union of feasible regions, it has to be compared pointwise with all the regions forming the union, i.e. the containment in the union can be checked via at most $2n$ vector comparisons of the type $d \le \overline{d}^{(k)}$ and $d \ge \underline{d}^{(k)}$. So, the overall complexity of checking feasibility grows linearly with the number of polytopes that form the full estimate of the feasibility region.

The operation of vector comparisons can be implemented in an extremely fast way on modern data-parallel hardware architectures. Therefore, it is possible to aggregate a database of an extremely high number of trajectories before the computational overhead of checking feasibility becomes comparable to other optimization or simulation procedures in the decision-making loop. Notably, the resulting feasibility set is defined in the gas withdrawal space, and does not depend either on the details of the power dispatch on generator side, nor on the topology of power system. Hence, the constructed database of certificates can be naturally reused in multiple gas-power coupling risk assessment studies. Moreover, whenever the resulting certificates for feasibility and infeasibility cover most of the interesting part of the phase space, they can be naturally used to estimate the risks of infeasibility even in the case of highly reliable systems with extremely low probability of crossing the boundary of the feasibility set.

## IV. Simulations

To validate the performance of the proposed algorithm, we have carried out a series of numerical experiments on a model described in Section II. The original model was modified to incorporate distributed renewable generation on all the gas consumption nodes corresponding to residential users. Intermittency and limited predictability of renewable generation was modeled as a stochastic component of the overall power demand. Because realistic modeling of renewable fluctuations is not the focus of this study, the simulations relied on a simplified model. Specifically, a random identically distributed component with uniform power distribution was added to the consumption vector at every hour and the resulting random time series was interpolated via a standard spline function. To assess the system performance in highly stressed conditions we assumed that the level of renewable penetration can be rather high, so the overall variability of the consumption vector was as high as $\pm 10\%$ of the base consumption.

The simulations were carried out for random samples of the renewable power production via the procedure described below. First, for a given forecast of gas consumption the optimal power flow and optimal gas flow problems were solved, following the procedures described in section II-B, which approximates the operation of modern power markets. After the optimal power dispatch and gas transmission policies were identified, a new sample of gas consumption was generated representing the actual consumption affected by random renewable power generation. Gas flow dynamics following the policies identified in the first step were modeled with the new consumption vector. In this sense, the simulations assumed a highly imperfect forecast and did not incorporate any adjustment of the compressor policies. This assumption,

although not critical for the mathematical foundation of the proposed algorithm, is certainly a simplification of the actual decision making policies. The feasibility was assessed using the pressure constraints on individual compression stations.

There can be vastly different policies for pressure regulation at compressor stations on the gas network side. In this study we relied on the simplest approach, in which constant compression factors are optimized based on the initial gas consumption forecast. In our simulation algorithm, we first sample from the random ensemble of power generations to produce an initial forecast of the gas withdrawals. The resulting continuous withdrawal is averaged over the whole time interval, and optimal compression factors are computed by using the static optimal gas flow approximation [15]. These compression factors were assumed to be fixed and not subject to any further change, even when the actual withdrawal vector differed strongly from the forecasted value. Fixed values of compression rates coupled with imperfect forecast can result in pressure overloads and consequently in shortages of gas availability to gas-fired power plants. We note that such phenomena are increasingly observed in gas transmission systems under stressed conditions [37].

To characterize the feasibility region of the gas withdrawal vector, dynamic simulations of gas flows were performed for individual realizations of distributed generation power outputs and the corresponding gas withdrawal rates that were found by solving the OPF problem. Even for highly stressed conditions, the probability of finding the infeasible fluctuation is vanishingly small. Hence, fast certificates of feasibility can greatly improve the computational efficiency of the risk assessment algorithm.

We have implemented a simplified version of the algorithm described in Section III. The feasibility region construction algorithm was linked to the "feasibility oracle" that accepted the gas withdrawal rates $d(t)$ as an input and reported whether the gas pressure limits were violated in dynamic simulations as the output. The bisection algorithm with 10 iterations was used to estimate the values of $\overline{\lambda}$ and $\underline{\lambda}$ with characteristic accuracy of $2^{-10} \approx 10^{-3}$.

To assess the effectiveness of the algorithm, we have generated multiple scenarios of renewable generation and associated withdrawal rates. For every scenario we have calculated the corresponding feasibility and infeasibility regions. A sample of 4 corresponding values of the $\overline{\lambda}$ and $\underline{\lambda}$ for $\pm 10\%$ renewable fluctuation magnitude are presented in the table below.

Table I
FEASIBILITY SET CHARACTERISTICS

| **Case** | $\underline{\lambda}$ | $\overline{\lambda}$ |
|---|---|---|
| 1 | 0.185 | 1.135 |
| 2 | 0.213 | 1.147 |
| 3 | 0.211 | 1.154 |
| 4 | 0.187 | 1.142 |

As one can see, the system generally operates with about 15% gas withdrawal margin. Moreover, fluctuations that result in anomalously high levels of distributed power generation that limit the need for natural gas do not cause any stress on the gas pipeline network.

We have found that the efficiency of certification was reasonably high for relatively small levels of renewable variability resulting in 5% of power consumption variations. In this case, the feasibility region for a randomly chosen scenario certified feasibility of about 8% of independently chosen scenarios. We observed that random generation of a relatively small number of certificates is sufficient to screen the majority of scenarios.

However, for variability of more than 10%, the probability that the certificate associated with gas withdrawal vector $d$ would certify feasibility of a randomly sampled vector $d'$ is smaller than 1%, so a large number of certificates need to be accumulated to achieve desired efficiencies. At the same time, only a few components of the vectors typically violated the inequalities. This observation suggests that advanced sampling procedures for selecting the most frequently violated components can significantly improve the performance of the algorithm. In this manuscript we did not experiment with possible sampling approaches. We plan to explore various strategies for constructing this set in future extensions of the present work, in which a more realistic model of the renewable fluctuations will also be implemented. This will ensure that the gas withdrawal rates are more realistic and provide insight about potential performance of the algorithm in real-life settings.

## V. Discussion and Conclusions

In this work we have analyzed the coupling of natural gas and electricity infrastructures. We have focused primarily on the task of characterizing the set of gas flow feasibility domains defined in the space of gas withdrawals. The monotone dependence of gas pipeline pressures at any point and time on preceding gas withdrawals allowed us to develop a powerful and efficient algorithm for constructively characterizing the set of domains in the space of gas withdrawals that are provably feasible and infeasible. The algorithm was validated through comparison with direct simulations of a detailed coupled infrastructure model that approximates the modern decision making process in the power and gas industry. In particular, the model accounts accurately for the transfer of mass and momentum in gas pipelines. Tests of our algorithm show that it is accurate and efficient even in the more challenging regime of weak coupling, when variability due to renewable energy resources is relatively small.

There are many natural applications of the proposed feasibility analysis to power system planning and operation. We list several below, and discuss further development steps.

- *Assessment of the gas supply disruption risk*. The proposed methodology provides an opportunity for ISOs to assess the risk of the gas supply disruption in the presence of uncertainty in intra-day gas withdrawal rates induced by intermittent renewable power sources. The key advantage of the methodology is in its natural modularity – complete decoupling of the three important computational processes: sampling from random renewable generation scenarios, simulation of power grid response to the scenarios, and, finally, simulation of the resulting gas pipeline network dynamics. This decoupling allows the power system operators to rely solely on receiving weather forecasts and gas network simulations from (possibly different) vendors, rather than getting it through complicated multi-domain simulation software and exchanging data with gas operators. Interaction between the three simulation modules is established via very simple interfaces. Sampling from random scenarios results in power generation/consumption time-series on the buses with high penetration of renewable sources. The gas system simulation acts as a so-called feasibility oracle that only provides information about the feasibility of the gas flow dynamics given fuel usage rates at gas-fired power plants. Coordinated execution of the modules, guided by the algorithm proposed in our work, results in an efficient and powerful tool for estimation of the feasibility set that could be naturally used to assess the risks in the system.
- *Gas-aware power grid operation and planning*. Gas flows are described by a system of complicated nonlinear partial differential equations, so that the actual feasibility region is extremely complex and does not admit any analytic characterization. Approximations of the feasibility region constructed using our technique have a very simple and geometrically transparent form, stated as a set of polytopes in the space of gas withdrawals. The simple description of the feasibility regions provides enables straightforward incorporation into existing power system toolboxes, including power solvers, generation dispatch, unit commitment optimizers, and software developed for transmission planning/expansion. Incorporation of these gas-related constraints would result in gas-aware optimization that is not burdened by significant computational overhead. Achievement of this ambitious goal requires more research on optimal construction of a more comprehensive (inclusive) description of the feasibility domain as a union of simple polytopes.
- *Coordinated operation of gas and power infrastructures*. Reaching high levels in future energy system reliability and resilience is not possible without coordinated operation of gas and electricity infrastructures. Apart from the obvious technical challenges, the problem is further complicated by the lack of regulatory policies encouraging data sharing and cooperation of gas and electricity operators. One way to achieve the desired levels of reliability without drastic changes to the current regulatory landscape lies in establishment of simple interfacial contracts that ensure reliable operation of both infrastructures. Simple domains in gas withdrawal vector space are a natural choice of such a contract. Properly formed feasibility regions in the gas withdrawal space can be adjoined as simple, even linear, constraints within commercial power system optimization software packages. These additional constraints would ensure that the gas pipeline infrastructure can operate without violation of any technological limits potentially resulting in failure of the equipment and cross-infrastructural cascading failure. On the other hand, power system operations could be naturally adapted to incorporate these feasibility regions as additional operational constraints. Whenever the regions are large enough, the extension of decision making will not have any major effect of overall operation costs. Such constraints will come into play at times of peak demand for both electricity and gas, at which time coordinated decision making would result in substantial economic benefits.

## REFERENCES


[1] K. W. Costello, "Exploiting the abundance of us shale gas: Overcoming obstacles to fuel switching and expanding the gas distribution system," *Energy LJ*, vol. 34, p. 541, 2013.

[2] R. Levitan *et al.*, "Pipeline to reliability: Unraveling gas and electric interdependencies across the eastern interconnection," *Power and Energy Magazine, IEEE*, vol. 12, no. 6, pp. 78–88, 2014.

[3] C. Sahin, M. Shahidehpour, and I. Erkmen, "Generation risk assessment in volatile conditions with wind, hydro, and natural gas units," *Applied Energy*, vol. 96, pp. 4–11, 2012.

[4] P. J. Hibbard and T. Schatzki, "The interdependence of electricity and natural gas: current factors and future prospects," *The Electricity Journal*, vol. 25, no. 4, pp. 6–17, 2012.

[5] T. Pugh and J. P. Blackford, "Implications of greater reliance on natural gas for electric generation," Tech. Rep., 2010.

[6] M. Shahidehpour and Z. Li, "White paper: Long-term electric and natural gas infrastructure requirements," llinois Institute of Technology, Tech. Rep., 2014.

[7] M. Chertkov, S. Backhaus, and V. Lebedev, "Cascading of fluctuations in interdependent energy infrastructures: Gas-grid coupling," *arxiv:1411.2111*, 2014.

[8] R. D. Tabors and S. Adamson, "Measurement of energy market inefficiencies in the coordination of natural gas & power," in *47th Hawaii Internat. Conf. on System Sci. (HICSS)*. IEEE, 2014, pp. 2335–2343.

[9] M. Chertkov, M. Fisher, S. Backhaus, R. Bent, and S. Misra, "Pressure fluctuations in natural gas networks caused by gas-electric coupling," in *2015 48th Hawaii International Conference on System Sciences (HICSS)*. IEEE, 2015, pp. 2738–2747.

[10] A. Lee, O. Zinaman, and J. Logan, "Opportunities for synergy between natural gas and renewable energy in the electric power and transportation sectors," National Renewable Energy Laboratory, Tech. Rep., 2012.

[11] MITEI. (2013) Growing concerns, possible solutions: The Interdependency of Natural Gas and Electricity Systems. [Online]. Available: http://mitei.mit.edu/publications/reports-studies/growing-concerns-possible-solutions

[12] A. Zlotnik, S. Dyachenko, S. Backhaus, and M. Chertkov, "Model reduction and optimization of natural gas pipeline dynamics," in *2015 ASME Dynamic Systems and Control Conference*, Columbus, OH, 2015.

[13] A. Zlotnik, M. Chertkov, and S. Backhaus, "Optimal control of transient flow in natural gas networks," in *54th IEEE Conference on Decision and Control*, Osaka, Japan, 2015.

[14] P. Wong and R. Larson, "Optimization of natural-gas pipeline systems via dynamic programming," *Automatic Control, IEEE Transactions on*, vol. 13, no. 5, pp. 475–481, 1968.

[15] S. Misra, M. W. Fisher, S. Backhaus, R. Bent, M. Chertkov, and F. Pan, "Optimal compression in natural gas networks: A geometric programming approach," *IEEE Transactions on Control of Network Systems*, vol. 2, no. 1, pp. 47–56, 2015.

[16] M. Vuffray, S. Misra, and M. Chertkov, "Monotonicity of dissipative flow networks renders robust maximum profit problem tractable: General analysis and application to natural gas flows," *Submitted to 54th IEEE Conference on Decision and Control*, 2015.

[17] G. Como, K. Savla, D. Acemoglu, M. Dahleh, E. Frazzoli *et al.*, "Robust distributed routing in dynamical networks – part i: Locally responsive policies and weak resilience," *IEEE Transactions on Automatic Control*, vol. 58, no. 2, pp. 317–332, 2013.

[18] C. Grigg *et al.*, "The IEEE reliability test system-1996. a report prepared by the reliability test system task force of the application of probability methods subcommittee," *IEEE Transactions on Power Systems*, vol. 14, no. 3, pp. 1010–1020, 1999.

[19] W. Katzenstein and J. Apt, "Air emissions due to wind and solar power," *Environmental science & technology*, vol. 43, no. 2, pp. 253–258, 2008.

[20] R. D. Zimmermann *et al.*, "Matpower: Steady-state operations, planning, and analysis tools for power systems research and education," *IEEE Trans. Power Systems*, vol. 23, no. 1, pp. 12–19, 2011.

[21] Forward Market Operations, "Energy & Ancillary Services Market Operations, M-11 Rev. 75," PJM, Tech. Rep., 2015.

[22] ISO New England, "ISO New England Manual for Market Operations, M-11 Rev. 49," ISONE, Tech. Rep., 2014.

[23] E. Litvinov, "Design and operation of the locational marginal prices-based electricity markets," *Generation, Transmission Distribution, IET*, vol. 4, no. 2, pp. 315–323, February 2010.

[24] M. Chaudry, J. Wu, and N. Jenkins, "A sequential monte carlo model of the combined gb gas and electricity network," *Energy Policy*, vol. 62, pp. 473–483, 2013.

[25] M. Chaudry, N. Jenkins, and G. Strbac, "Multi-time period combined gas and electricity network optimisation," *Electric Power Systems Research*, vol. 78, no. 7, pp. 1265–1279, 2008.

[26] T. Li, M. Eremia, and M. Shahidehpour, "Interdependency of natural gas network and power system security," *IEEE Transactions on Power Systems*, vol. 23, no. 4, pp. 1817–1824, 2008.

[27] C. Liu, M. Shahidehpour, Y. Fu, and Z. Li, "Security-constrained unit commitment with natural gas transmission constraints," *IEEE Transactions on Power Systems*, vol. 24, no. 3, pp. 1523–1536, 2009.

[28] C. Liu, M. Shahidehpour, and J. Wang, "Coordinated scheduling of electricity and natural gas infrastructures with a transient model for natural gas flow," *Chaos: An Interdisciplinary Journal of Nonlinear Science*, vol. 21, no. 2, p. 025102, 2011.

[29] B. Stott, J. L. Marinho, and O. Alsac, "Review of linear programming applied to power system rescheduling," in *Power Industry Computer Applications Conference, 1979. PICA-79. IEEE Conference Proceedings*, May 1979, pp. 142–154.

[30] M. D. Ilic and J. Zaborszky, *Dynamics and control of large electric power systems*. Wiley New York, 2000.

[31] J. Ruths, A. Zlotnik, and J.-S. Li, "Convergence of a pseudospectral method for optimal control of complex dynamical systems," in *50th IEEE Conf. on Decision and Control*. IEEE, 2011, pp. 5553–5558.

[32] L. Biegler and V. Zavala, "Large-scale nonlinear programming using IPOPT: An integrating framework for enterprise-wide dynamic optimization," *Computers & Chem. Eng.*, vol. 33, no. 3, pp. 575–582, 2009.

[33] A. Thorley and C. Tiley, "Unsteady and transient flow of compressible fluids in pipelines – a review of theoretical and some experimental studies," *Internat. J. of Heat and Fluid Flow*, vol. 8, pp. 3–15, 1987.

[34] M. Herty, J. Mohring, and V. Sachers, "A new model for gas flow in pipe networks," *Math. Methods in the Applied Sci.*, vol. 33, no. 7, pp. 845–855, 2010.

[35] A. Osiadacz, "Simulation of transient gas flows in networks," *International J. for Numerical Methods in Fluids*, vol. 4, pp. 13–24, 1984.

[36] C. Borraz-Sanchez, "Optimization methods for pipeline transportation of natural gas," Ph.D. dissertation, Bergen Univ.(Norway), 2010.

[37] "Tennessee gas pipeline company ISO NE presentation: March 24, 2011," http://iso-ne.com/committees/comm_wkgrps/othr/egoc/mtrls/2011/mar302011/el_paso_isone_necpuc_032411.pdf.